
Article:
Hodono, S., Shimokawa, A., Stewart, N.J. orcid.org/0000-0001-8358-394X et al. (6 more authors) (2018) Ethyl pyruvate improves pulmonary function in mice with bleomycin-induced lung injury as monitored with hyperpolarized 129Xe MR imaging. Magnetic Resonance in Medical Sciences, 17 (4). pp. 331-337. ISSN 1347-3182

https://doi.org/10.2463/mrms.mp.2017-0163

Magn Reson Med Sci 2018; 17; 331–337
doi:10.2463/mrms.mp.2017-0163
Published Online: March 9, 2018

MAJOR PAPER

Ethyl Pyruvate Improves Pulmonary Function in Mice with Bleomycin-induced Lung Injury as Monitored with Hyperpolarized ^{129}Xe MR Imaging

Shota Hodono[1], Akihiro Shimokawa[1], Neil J. Stewart[2], Yukiko Yamauchi[1], Renya Nishimori[1], Mami Yamane[1], Hirohiko Imai[3], Hideaki Fujiwara[1], and Atsuomi Kimura[1*]

Purpose: High Mobility Group Box1 (HMGB1), which is one of the damage-associated molecular pattern molecules relating to various inflammatory diseases, has gained interest as a therapeutic target because of its involvement in wound healing processes. In the present study, we investigated HMGB1 as a potential therapeutic target in a model of lung fibrosis using a preclinical hyperpolarized ^{129}Xe (HPXe) MRI system.
Methods: Lung injury was induced by intra-peritoneal injection of bleomycin (BLM) in 19 mice. Three weeks post-injection (when fibrosis was confirmed histologically), administration of ethyl pyruvate (EP) and alogliptin (ALG), which are down- and up-regulators of HMGB1, respectively, was commenced in six and seven of the 19 mice, respectively, and continued for a further 3 weeks. A separate sham-instilled group was formed of five mice, which were administered with saline for 6 weeks. Over the second 3-week period, the effects of disease progression and pharmacological therapy in the four groups of mice were monitored by HPXe MRI metrics of fractional ventilation and gas-exchange function.
Results: Gas-exchange function in BLM mice was significantly reduced after 3 weeks of BLM challenge compared to sham-instilled mice ($P < 0.05$). Ethyl pyruvate was found to improve HPXe MRI metrics of both ventilation and gas exchange, and repair tissue damage (assessed histologically), to a similar level as sham-instilled mice ($P < 0.05$), whilst ALG treatment caused no significant improvement of pulmonary function.
Conclusion: This study demonstrates the down-regulator of HMGB1, EP, as a potential therapeutic agent for pulmonary fibrosis, as assessed by a non-invasive HPXe MRI protocol.

Keywords: *ethyl pyruvate, High Mobility Group Box1, hyperpolarized ^{129}Xe magnetic resonance imaging, murine bleomycin-induced lung fibrosis, therapeutic target*

Introduction

In recent years, hyperpolarized (HP) noble gas MRI has been developed as a powerful tool for functional imaging of lung.[1,2] In particular, hyperpolarized ^{129}Xe (HPXe) MRI can be applied to a wide range of disease phenotypes since it affords information about gas exchange in addition to ventilation function. Sensitivity to gas exchange arises from the fact that HPXe dissolves in alveolar tissue and blood and exhibits a distinct chemical shift from that of gaseous-phase HPXe in the lung airspaces.

We have developed a home-built continuous-flow type Xe polarizer for production of HPXe for preclinical applications, which allows the acquisition of functional images of the lung from spontaneously breathing mice using a preclinical MRI system.[3] Previously, we used this system to evaluate the efficacy of the drug ethyl pyruvate (EP) for treating chronic obstructive pulmonary disease (COPD).[4] In that study, we suggested that High Mobility Group Box1 (HMGB1), which is one of the damage-associated molecular patterns (DAMPs), is involved in COPD disease progression.

The HMGB1 is known to play a crucial role in various inflammatory lung diseases, including COPD.[5,6] When HMGB1 released from necrotic or apoptotic cells binds to its

[1]Department of Medical Physics and Engineering, Division of Medical Technology and Science, Faculty of Health Science, Graduate School of Medicine, Osaka University, 1-7 Yamadaoka, Suita, Osaka 565-0871, Japan
[2]Division of Bioengineering and Bioinformatics, Graduate School of Information Science and Technology, Hokkaido University, Hokkaido, Japan
[3]Department of Systems Science, Graduate School of Informatics, Kyoto University, Kyoto, Japan
*Corresponding author, Phone: +81-6-6879-2478,
E-mail: kimura@sahs.med.osaka-u.ac.jp

Received: November 10, 2017 | Accepted: February 7, 2018

receptors, which are receptor for advanced glycation end (RAGE) products, and toll-like receptors (TLRs) 2 and 4, it activates the transcription factor nuclear factor-kappa B (NF-κB) and mitogen-activated protein kinase (MAPK) signaling pathways, as shown in Fig. 1.[7–9] Somewhat paradoxically, a moderate expression of HMGB1 has been shown to be linked to wound healing processes through the activation of extracellular signal-regulated kinase (ERK) 1/2 involved in the MAPK pathway, while its overexpression exacerbates inflammation and pathology through NF-κB activation.[10] Ethyl pyruvate has previously been reported to dose-dependently activate ERK 1/2 through inhibition of HMGB1.[11–14] Combining these facts with our previous observations of EP treatment efficacy for a murine COPD model stated above, we hypothesized that EP could show therapeutic efficacy for other lung diseases via wound healing effects by ERK 1/2 activation, following anti-inflammatory responses by NF-κB down-regulation.

Pulmonary fibrosis is characterized by progressive and irreversible scar formation and alveolar septal wall thickening, which lead to severe respiratory dysfunction and ultimately death. Steroids and immunosuppressants have been found to be ineffective for improving prognosis.[15] At present, two novel drugs, nintedanib and pirfenidone, which have shown efficacy for slowing the decline of lung function, are still in a regime of conditional recommendation against use.[16] As such, preclinical studies have been actively pursued in order to develop novel therapeutic drugs using animal models of fibrosis, such as bleomycin (BLM)-challenge for mice.[17,18] In recent studies, the transforming growth factor-β1 (TGF-β1) involved in the Smad signaling pathway has been widely investigated as a potential therapeutic target.[19–20] However, to the best of our knowledge, there exist only one study reporting on the involvement of HMGB1 and the effect of EP in lung fibrosis progression, in which wound healing was not investigated.[11]

In the present study, we monitored the response of pulmonary function to treatment with EP in a BLM mouse model of fibrosis by HPXe MRI, following the non-invasive preclinical MRI protocol presented in Ref. 4. Additionally, in order to further investigate the relationship between HMGB1 and ERK 1/2 expression in disease and treatment processes, the efficacy of a Dipeptidyl Peptidase-4 (DPP-4) inhibitor, alogliptin (ALG), was also monitored because ALG is known to down-regulates ERK 1/2 expression probably through the inhibition of endogenous HMGB1 protease, DPP4.[21,22] The results were compared to support the involvement of ERK 1/2 expression in wound healing processes.

Methods

Animal preparation

All experimental and animal care procedures conformed to the guidelines of Osaka University.

A total of 24 male, 6-week-old, ddY mice weighing 30–35 g were purchased from Japan SLC, Inc. (Shizuoka, Japan). Mice were divided into four groups: 1) sham-instilled group (N = 5), 2) BLM-challenged group (N = 6), 3) EP-treated group (N = 6), and 4) ALG-treated group (N = 7). To induce fibrotic lung injury, a 75 μL saline solution of BLM (1.2 U/kg body weight; Sigma-Aldrich, St Louis, MO, USA) was intratracheally administrated to each mouse of the BLM-challenged, EP- and ALG-treated groups, while the sham-instilled mice were intratracheally administered with a 75 μL saline solution.[23] Three weeks after BLM-challenge, EP and ALG administration was commenced in the EP- and ALG-treated group, respectively, following a similar protocol to that in Ref. 4. Briefly, a 40 μL solution of EP (2.6 mg/kg body weight; Tokyo Chemical Industry Co., Ltd, Tokyo, Japan) or ALG (200 mg/kg body weight; Takeda Pharmaceutical Co., Ltd, Osaka, Japan) in saline was administered to each mouse in the EP- or ALG-treated group every weekday for an additional 3 weeks. Therefore, in total, 6 weeks were required to prepare the EP- and ALG-treated groups. The sham-instilled mice were intratracheally administered with 40 μL saline solution every weekday for the additional 3 week period, in order to ensure the same instillation process for all mice. In all cases, mice were anesthetized with 2% isoflurane (ISOFLU; Sumitomo Dainippon Pharma Co. Ltd, Osaka, Japan) prior to instillation. The survival rates of the whole 6-week procedure were 100%, 100%, 86%, and 100% for BLM-challenged, EP-treated, ALG-treated and sham-instilled groups, respectively.

Magnetic resonance imaging

The MRI measurements of all groups were performed at 3, 4, 5, and 6 weeks after commencement of saline or BLM

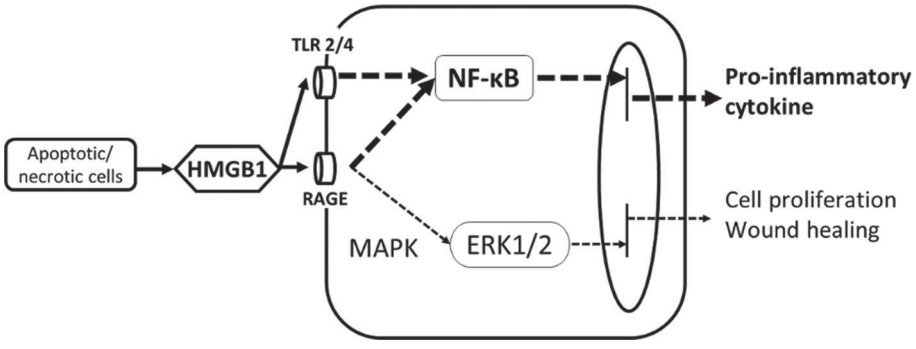

Fig. 1 Schematic representation of the extra-cellular production of High Mobility Group Box1, its subsequent binding with receptors receptor for advanced glycation end and toll-like receptors 2/4, and the corresponding activation of cellular signaling pathways. ERK, signal-regulated kinase; HMGB1, High Mobility Group Box1; MAPK, mitogen-activated protein kinase; NF-κB, factor-kappa B; RAGE, receptor for advanced glycation end; TLR, toll-like receptor.

challenge (i.e., for EP- and ALG-treated groups; 0, 1, 2, and 3 weeks from commencement of EP or ALG treatment). Immediately before all MR measurements, mice were anesthetized with 2% isoflurane, and non-invasive respiratory-gated imaging was performed without tracheal intubation.

All MRI measurements were performed on an Agilent Unity INOVA 400WB high-resolution NMR system equipped with VNMR 6.1C software (Agilent Technologies, Inc., Santa. Clara, CA, USA). To acquire respiratory-gated images from spontaneously breathing mice, the protocol described previously was used.[4] A respiratory sensor was employed to synchronize the acquisition of HPXe lung images with inspiratory or expiratory phases.

A home-built continuous-flow type ^{129}Xe polarizer was used to produce HPXe.[24] A gas mixture of HPXe and N_2 (Xe in natural abundance, ^{129}Xe fraction 0.26: 70%, N_2: 30%) was continuously delivered to the mouse in the MRI scanner at a flow rate of 50 mL/min. Mice spontaneously breathed the polarized gas after it was mixed with O_2 (flow rate 9 ml/min). Hyperpolarized ^{129}Xe images were acquired using a balanced steady-state free precession sequence modified by adding four 180°-pulses or two 90°-pulses in order to extract information about pulmonary gas-exchange or ventilation function, as described previously.[4,25] Acquisition parameters are replicated here for completeness: 1000-μs Gaussian-shaped radio-frequency (RF) pulse of flip angle α = 40°; acquisition bandwidth, 88 kHz; TR/TE = 3.6 ms/1.8 ms; echo train length, 8; number of shots, 4; number of averages, 8; coronal slice thickness, 20 mm; matrix, 64 × 32 with a FOV of 80 × 25 mm^2.

Pulmonary functional evaluation by HPXe MRI

Metrics of fractional ventilation, r_a and xenon gas exchange rate, f_D, of HPXe were evaluated as reported previously.[4] Only brief details are reproduced here for completeness.

First, r_a the alveolar volume fraction of gas turned over in a single breath, was evaluated. After gas-phase HPXe magnetization in the lung was destroyed by a saturation prepulse, a set of inspiratory images was acquired after n breathing cycles. Value n was incremented from 1 to 10 in steps of one, and then to 12, 15, and 20; in total, 13 images were acquired. From these images, a r_a map was obtained by pixel-by-pixel linear least squares fitting of the signal intensity as a function of n, using in-house MATLAB (The MathWorks, Inc., Natick, MA, USA) routines.

The xenon polarization transfer contrast (XTC) method was used to evaluate the parameter f_D, the rate of HPXe magnetization diffusing from the gas-phase to dissolved-phase within a given exchange time.[26] The XTC measurement was performed at the end-expiratory phase, and an f_D map was derived by pixel-by-pixel analysis using in-house MATLAB routines as for r_a.

Finally, r_a or f_D maps were reprocessed with a 2 × 2 median filter, and r_a or f_D values were averaged over the whole of the lungs for each mouse.

Histology

After HPXe MR measurements were completed, mice were killed with a lethal dose of carbon monoxide gas. Lungs were extracted, immersed in 10% formalin at 25 cmH_2O and processed for histology by staining with hematoxylin and eosin (H&E). Slides were evaluated to assess morphological changes in the lungs after 6 weeks. Coronal H&E-stained lung images were obtained from each mouse. Five regional images (right upper, middle and lower lobes, and upper and lower regions of the left lung, each of dimensions 175 μm × 131.25 μm) were then captured from each coronal slide using a digital microscope (Celestron LCD Microscope PRO <CE44345>; Celestron, LLC., Torrance, CA, USA). Septal wall thickness, h (μm), values were calculated in the five regions from four separate slices and averaged for each mouse. All digital images were processed using ImageJ (National Institutes of Health, Bethesda, MD, USA).

In order to monitor morphological changes induced 3 weeks after BLM administration (i.e., the beginning of MRI measurements), an additional histological analysis group (HA_3w, N = 5 mice) was prepared 3 weeks post-BLM-challenge using the same protocol as described above.

Statistical analysis

Statistical analysis was performed by one-way analysis of variance (ANOVA) with Tukey–Kramer post-hoc analysis to identify differences between groups. All data are presented as mean ± standard deviation (SD) or box-and-whisker plots, and differences are considered significant at the $P < 0.05$ level.

Results

Figure 2 displays representative, Fig. 2a f_D and Fig. 2b r_a maps obtained from the sham-instilled, BLM-challenged, EP-treated, and ALG-treated groups. Figure 3 shows longitudinal changes in the group-mean values of f_D and r_a, respectively, at 3–6 weeks post-BLM or saline challenge. The administration of EP and ALG was commenced at week 3, when a significant decrease of mean f_D value for BLM-challenged (4.8 ± 1.0), EP-treated ($f_{D\text{—EP-treated}}$ = 4.8 ± 0.8) and ALG-treated ($f_{D\text{—ALG-treated}}$ = 4.8 ± 1.4) groups compared to that of the sham-instilled group ($f_{D\text{—sham-instilled}}$ = 7.4 ± 1.1) was observed ($P < 0.05$). The mean f_D value of the EP-treated group gradually increased over the course of the treatment and was significantly larger ($f_{D\text{—EP-treated}}$ = 6.8 ± 0.8) than that of the BLM-challenged group ($f_{D\text{—BLM–challenged}}$ = 4.3 ± 0.9) at week 6 ($P < 0.05$), while the BLM-challenged group showed relatively little change in f_D during the whole observation period. On the other hand, the mean f_D values of the ALG-treated group at weeks 5 and 6 were still significantly smaller than those of the sham-instilled group.

The mean r_a value of the EP-treated group was ($r_{a\text{—EP-treated}}$ = 0.24 ± 0.02) at week 6, a significant improvement compared with week 3 ($r_{a\text{—EP-treated}}$ = 0.20 ± 0.02) ($P < 0.05$)

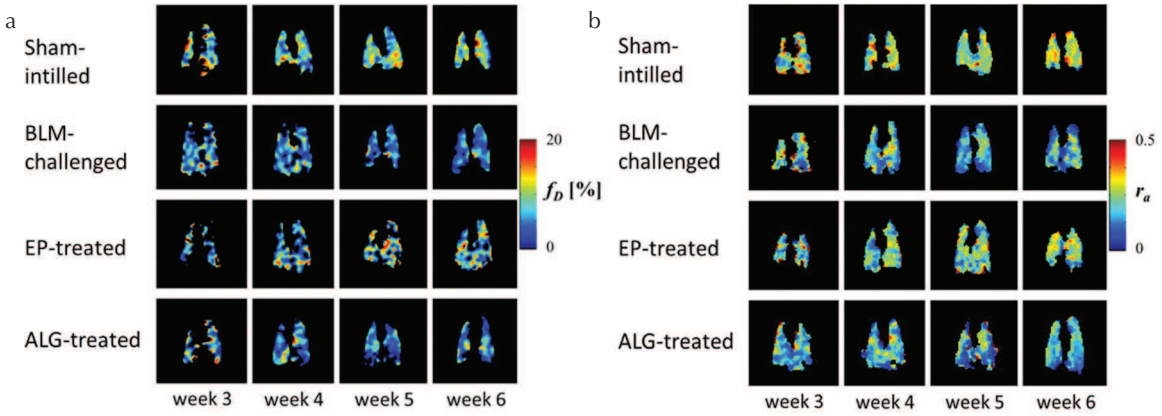

Fig. 2 Representative parametric maps of (**a**) f_D and (**b**) r_a derived from longitudinal studies of mice in each of the four groups, from top to bottom: sham-instilled; bleomycin (BLM)-challenged; ethyl pyruvate (EP)-treated; alogliptin (ALG)-treated. In all cases, the horizontal direction shows the time course from the initial intra-tracheal injection of BLM or saline.

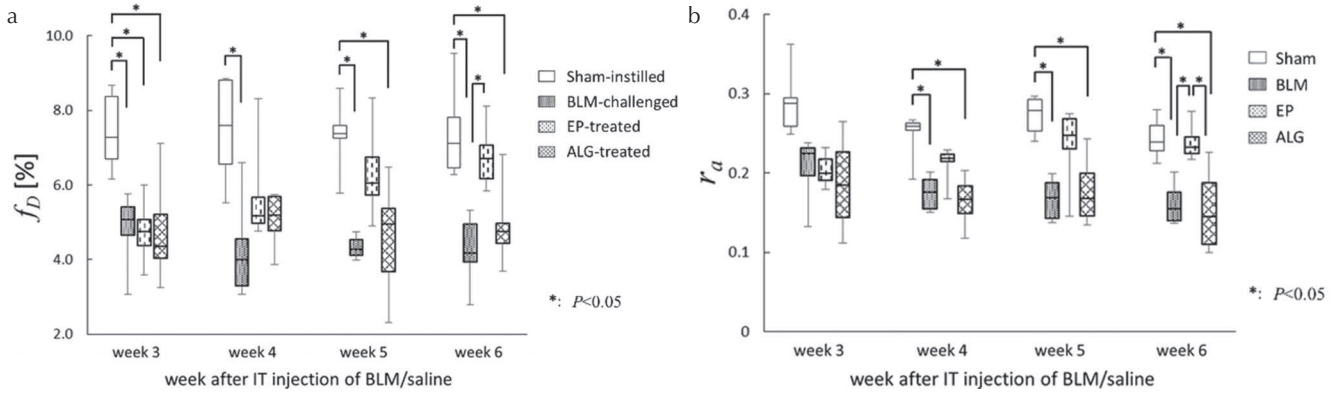

Fig. 3 Box plots of the temporal change of mean (**a**) f_D and (**b**) r_a values for all mice, separated by group, as a function of time post-intra-tracheal injection of bleomycin or saline. Significant differences between groups are indicated by solid lines (*: $P < 0.05$). ALG, alogliptin; BLM, bleomycin; EP, ethyl pyruvate; IT, intra tracheal.

and larger than that of the BLM-challenged and ALG-treated groups ($r_{a\_\text{BLM-challenged}} = 0.16 \pm 0.03$, $r_{a\_\text{ALG-treated}} = 0.15 \pm 0.05$, respectively) ($P < 0.05$). The mean r_a value of the ALG-treated group remained low compared with the sham-instilled group, i.e., at a similar level to that of the BLM-challenged group, at weeks 4–6.

Figure 4a depicts group-mean values of the septal wall thickness, h, and Fig.4b representative histological results for all groups including the histological analysis group (HA_3w). The mean h value of the HA_3w group (mice killed after 3 weeks of BLM-challenge) was $h_{\text{HA\_3w}} = 10.8 \pm 1.7$ μm, significantly larger than that of the sham-instilled mice at the same time-point ($P < 0.05$). Similarly, terminal (6-week) h values of BLM and ALG-treated groups ($h_{\_\text{BLM-challenged}} = 10.8 \pm 1.9$ μm and $h_{\_\text{ALG-treated}} = 11.6 \pm 1.6$ μm) were larger than that of the sham-instilled group ($h_{\_\text{sham-instilled}} = 6.4 \pm 0.7$ μm, $P < 0.01$), while the mean h of the EP-treated group was significantly smaller than that of both the BLM and ALG-treated groups ($h_{\_\text{EP-treated}} = 7.6 \pm 1.0$ μm, $P < 0.05$) and comparable to that of the sham-instilled group ($P > 0.05$).

Figure 5 shows the correlations between MRI metrics of lung function and the histological h value, evaluated at week 6. A significant, positive correlation was found between r_a and f_D ($P < 0.001$), while negative correlations were found between h and f_D, and h and r_a ($P < 0.001$).

Discussion

In the present study, the temporal changes of pulmonary ventilation and gas-exchange function in mice treated with EP and ALG as therapeutic agents for BLM-induced lung injury were monitored by HPXe MRI for 3 weeks, treatment commencing 3 weeks post-BLM-challenge. According to Moeller et al,[17] the efficacy of anti-fibrotic agents should be evaluated at least 7 days after BLM-challenge and in the phase of established fibrosis rather than the phase of inflammation. In our measurements, week 3 was determined as the point where sufficient symptoms of fibrosis were observed; a significant decrease of the mean f_D values for the BLM-challenged, EP-treated and ALG-treated groups compared to

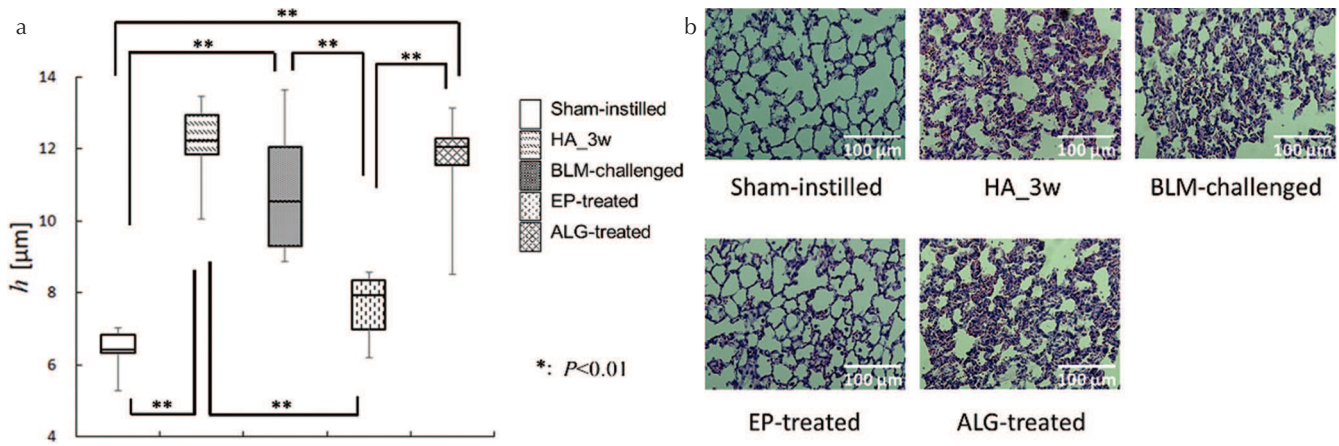

Fig. 4 (**a**) Box plots of the mean septal wall thickness (*h*) obtained from mice in each of the five groups, from left to right: sham-instilled; histological analysis (HA_3w), bleomycin -challenged; ethyl pyruvate-treated; alogliptin-treated. (**b**) Representative examples of hematoxylin and eosin stained histology slides obtained from each group. ALG, alogliptin; BLM, bleomycin; EP, ethyl pyruvate.

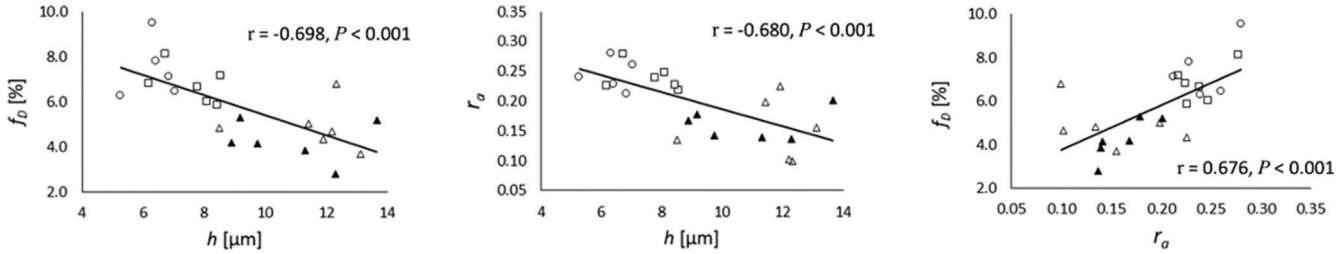

Fig. 5 Correlations between hyperpolarized ^{129}Xe (HPXe) MRI-derived parameters of pulmonary function (r_a and f_D), and histology-derived septal wall thickness (*h*) obtained from the sham-instilled (□), bleomycin-challenged (▲), ethyl pyruvate-treated (○), and alogliptin-treated (△) groups after the 6-week experimental protocol. Pearson's *r* values and *P* values of statistical significance are noted in each plot.

that of the sham-instilled group. This choice was supported by histological measurements of significantly elevated *h* in the HA_3w group. Therefore, the administration of EP was commenced from this time-point. However, we note one report in which EP treatment was investigated for 2 weeks after only 3 days of BLM-challenge,[11] thus, the choice of timing for commencement of fibrosis treatment is still a matter of debate.

At week 4, both f_D and r_a values tended to be slightly lower than those at week 3; however, after week 4, both metrics remained approximately constant for the BLM-challenged group (i.e., the absolute values of the metrics did not significantly degrade for the remainder of the observation period) ($f_{D\_\text{BLM-challenged\_3w}} = 4.8 \pm 1.0$ vs. $f_{D\_\text{BLM-challenged\_6w}} = 4.3 \pm 0.9$, $r_{a\_\text{BLM-challenged\_3w}} = 0.21 \pm 0.04$ vs. $r_{a\_\text{BLM-challenged\_6w}} = 0.16 \pm 0.03$). However, it should be recalled that a typical feature of BLM-induced lung injury is partial reversibility of pathology over time[15]; initially, fibrosis occurs following an acute inflammation stage with the expression of signals such as TGF-β1, but subsequently, the inflammatory reactions gradually disappear and the pathology proceeds with fibrotic lung remodeling.[27,28] Babin et al. reported that inflammation in a rat model was markedly attenuated after 21 days of BLM-challenge.[29] Therefore, our observations suggest the acute inflammatory reaction attenuated over time, but since fibrosis was already established around weeks 3–4, f_D and r_a did not change significantly (i.e., implying that fibrosis predominantly determines the pulmonary functional status and is irreversible, as expected).

The observation of a significant correlation of f_D and r_a values at week 6 (Fig. 5) suggests the BLM model acted to simultaneously impair both ventilation and gas-exchange function. Previously, we reported that reductions in f_D and r_a were indicative of septal wall destruction and bronchial wall thickening for a murine COPD model.[4] In that study, the reduction in f_D correlated with both septal wall and bronchial wall thicknesses, while r_a correlated with bronchial wall thickening only. Conversely, in the present study, both metrics were shown to be related to septal wall thickening associated with fibrotic lung remodeling (Fig. 5).

Longitudinal observation of f_D and r_a enabled quantification of the treatment efficacy of EP. The BLM-induced low f_D and r_a values at week 3 were recovered to a similar level as the sham-instilled group by 3 week's administration of EP ($f_{D\_\text{EP-treated\_6w}} = 6.8 \pm 0.8$, $f_{D\_\text{sham-instilled\_6w}} = 7.4 \pm 1.3$ and $r_{a\_\text{EP-treated\_6w}} = 0.24 \pm 0.02$, $r_{a\_\text{sham-instilled\_6w}} = 0.24 \pm 0.03$, respectively). Since the administration of EP was commenced after 3 weeks of BLM-challenge (i.e., after a significant impairment of pulmonary function was observed),

we believe that the measured action of EP was indeed therapeutic rather than preventative against BLM-induced lung injury.

Ethyl pyruvate is known to down-regulate the HMGB1 level through NF-κB inhibition, and moderately up-regulate ERK 1/2 expression downstream of the HMGB1/RAGE signaling pathway.[14,30,31] Hence, the action of EP provides some insight into the involvement of HMGB1 and ERK 1/2 in fibrosis development via the BLM model as shown in Fig. 6a. According to Ebina et al., gradual increase of HMGB1 expression after the inflammatory response stage exacerbates fibrosis.[32] Ethyl pyruvate administration may ameliorate this fibrotic pathology by down-regulation of HMGB1 and up-regulation of ERK 1/2, the latter which is reportedly involved in tissue repair processes.[10] It is also worth noting that Yupingfeng, a Chinese herbal remedy for respiratory ailments, has been found to inhibit HMGB1, which caused a reduction in TGF-β1 production and subsequently diminished collagen deposition in a BLM model of pulmonary fibrosis.[33]

In the present study, the septal wall thickness, h, of the EP-treated group was found to be significantly smaller than that of the BLM-challenged group (Fig. 4). This result, combined with the recovery of mean f_D and r_a suggests that the EP therapy directly acted against fibrotic tissue damage via ERK 1/2 activation and led to the recovery of pulmonary function in BLM-challenged mice. In order to further elucidate the involvement of ERK 1/2 in tissue repair processes, ALG was administered to BLM-challenged mice, since it is known to down-regulate ERK 1/2 (i.e., opposite to EP) probably through the inhibition of endogenous HMGB1 protease, DPP-4 (Fig. 6b).[21,22] A positive treatment response with ALG was not observed; the longitudinal changes in mean f_D and r_a of the ALG-treated group showed similar tendency to those of the BLM-challenged group, and the h value of the ALG-treated group was comparable to the BLM-challenged group and significantly larger than that of the sham-instilled group. These findings indicate that ALG did not act to repair lung tissue damage induced by BLM by ERK 1/2 deactivation and hence caused no significant changes in pulmonary function during the observation period (Fig. 3). In conclusion, we propose that the observed efficacy of EP for BLM-induced lung injury is mediated by regulation of HMGB1 and ERK 1/2 expression. EP is reported to have low toxicity and to be safe at clinically relevant doses, and has recently been enrolled in preliminary clinical trials.[34] As such, we believe our results are of particular interest to pulmonologists, and scientists and clinicians involved in human pulmonary MRI.

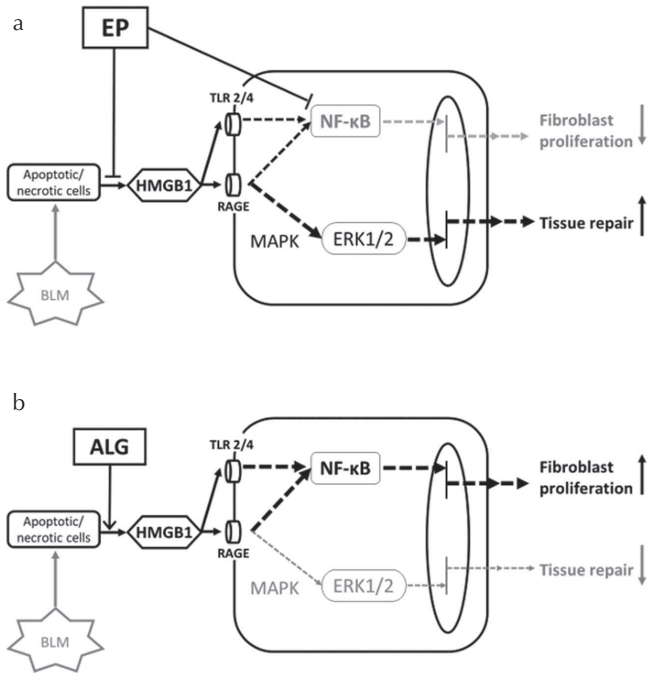

Fig. 6 Proposed contribution of ethyl pyruvate (EP) to fibrosis therapy in the bleomycin model of lung fibrosis. (**a**) Ethyl pyruvate down-regulates the HMGB1 expression through NF-κB inhibition and moderately activates ERK 1/2, thereby initiating wound healing process. (**b**) ALG, which up-regulates the HMGB1 expression and deactivates ERK 1/2, did not show a positive effect for fibrosis therapy. BLM, bleomycin; MAPK, mitogen-activated protein kinase; NF-κB, factor-kappa B; RAGE, receptor for advanced glycation end; TLR, toll-like receptors.

Conclusion

In the present study, the efficacy of EP and ALG treatment for BLM-induced lung fibrosis has been investigated by a preclinical HPXe MRI protocol that can easily be applied to assessment of other diseases and novel drug targets. EP treatment was found to improve ventilation and gas-exchange impairment and repair tissue damage associated with lung fibrosis, whilst ALG caused no significant change in pulmonary structure or function. The present results suggest that the inhibition of NF-κB with EP results in regulation of HMGB1 and ERK1/2 expression, thereby leading to therapeutic efficacy.

Acknowledgments

This work was supported by the Japan Society for the Promotion of Science (JSPS) KAKENHI grant number, JP15H03006. NJS is an International Research Fellow of the JSPS.

Conflicts of Interest

The authors declare that they have no conflicts of interest.

References

1. Ebner L, Kammerman J, Driehuys B, Schiebler ML, Cadman RV, Fain SB. The role of hyperpolarized ^{129}xenon in MR imaging of pulmonary function. Eur J Radiol 2017; 86:343–352.

2. Adamson EB, Ludwig KD, Mummy DG, Fain SB. Magnetic resonance imaging with hyperpolarized agents: methods and applications. Phys Med Biol 2017; 62:R81–R123.
3. Imai H, Kimura A, Fujiwara H. Small animal imaging with hyperpolarized ^{129}Xe magnetic resonance. Anal Sci 2014; 30:157–166.
4. Kimura A, Yamauchi Y, Hodono S, et al. Treatment response of ethyl pyruvate in a mouse model of chronic obstructive pulmonary disease studied by hyperpolarized ^{129}Xe MRI. Magn Reson Med 2017; 78:721–729.
5. Gangemi S, Casciaro M, Trapani G, et al. Association between HMGB1 and COPD: a systematic review. Mediators Inflamm 2015; 2015:164913.
6. Ding J, Cui X, Liu Q. Emerging role of HMGB1 in lung diseases: friend or foe. J Cell Mol Med 2017; 21:1046–1057.
7. Musumeci D, Roviello GN, Montesarchio D. An overview on HMGB1 inhibitors as potential therapeutic agents in HMGB1-related pathologies. Pharmacol Ther 2014; 141:347–357.
8. Zhang Y, Li S, Wang G, et al. Changes of HMGB1 and sRAGE during the recovery of COPD exacerbation. J Thorac Dis 2014; 6:734–741.
9. Wang H, Yang H, Czura CJ, Sama AE, Tracey KJ. HMGB1 as a late mediator of lethal systemic inflammation. Am J Respir Crit Care Med 2001; 164:1768–1773.
10. Lee DE, Trowbridge RM, Ayoub NT, Agrawal DK. High-mobility group box Protein-1, matrix metalloproteinases, and vitamin D in keloids and hypertrophic scars. Plast Reconstr Surg Glob Open 2015; 3:e425.
11. Hamada N, Maeyama T, Kawaguchi T, et al. The role of high mobility group box1 in pulmonary fibrosis. Am J Respir Cell Mol Biol 2008; 39:440–447.
12. Davé SH, Tilstra JS, Matsuoka K, et al. Ethyl pyruvate decreases HMGB1 release and ameliorates murine colitis. J Leukoc Biol 2009; 86:633–643.
13. Yu Y, Yu Y, Liu M, et al. Ethyl pyruvate attenuated coxsackievirus B3-induced acute viral myocarditis by suppression of HMGB1/RAGE/NF-κB pathway. Springerplus 2016; 5:215.
14. Kung CW, Lee YM, Cheng PY, Peng YJ, Yen MH. Ethyl pyruvate reduces acute lung injury via regulation of iNOS and HO-1 expression in endotoxemic rats. J Surg Res 2011; 167:e323–331.
15. Raghu G, Collard HR, Egan JJ, et al.; ATS/ERS/JRS/ALAT Committee on Idiopathic Pulmonary Fibrosis. An official ATS/ERS/JRS/ALAT statement: idiopathic pulmonary fibrosis: evidence-based guidelines for diagnosis and management. Am J Respir Crit Care Med 2011; 183:788–824.
16. Raghu G, Rochwerg B, Zhang Y, et al.; American Thoracic Society; European Respiratory Society; Japanese Respiratory Society; Latin American Thoracic Association. An official ATS/ERS/JRS/ALAT clinical practice guideline: treatment of idiopathic pulmonary fibrosis. an update of the 2011 clinical practice guideline. Am J Respir Crit Care Med 2015; 192: e3–e19.
17. Moeller A, Ask K, Warburton D, Gauldie J, Kolb M. The bleomycin animal model: a useful tool to investigate treatment options for idiopathic pulmonary fibrosis? Int J Biochem Cell Biol 2008; 40:362–382.
18. Srour N, Thébaud B. Mesenchymal stromal cells in animal bleomycin pulmonary fibrosis models: a systematic review. Stem Cells Transl Med 2015; 4:1500–1510.
19. Tanaka KI, Niino T, Ishihara T, et al. Protective and therapeutic effect of felodipine against bleomycin-induced pulmonary fibrosis in mice. Sci Rep 2017; 7:3439.
20. Ji Y, Dou YN, Zhao QW, et al. Paeoniflorin suppresses TGF-β mediated epithelial-mesenchymal transition in pulmonary fibrosis through a Smad-dependent pathway. Acta Pharmacol Sin 2016; 37:794–804.
21. Ta NN, Li Y, Schuyler CA, Lopes-Virella MF, Huang Y. DPP-4 (CD26) inhibitor alogliptin inhibits TLR4-mediated ERK activation and ERK-dependent MMP-1 expression by U937 histiocytes. Atherosclerosis 2010; 213:429–435.
22. Marchetti C, Di Carlo A, Facchiano F, et al. High mobility group box 1 is a novel substrate of dipeptidyl peptidase-IV. Diabetologia 2012; 55:236–244.
23. Namba T, Tanaka KI, Ito Y, et al. Induction of EMT-like phenotypes by an active metabolite of leflunomide and its contribution to pulmonary fibrosis. Cell Death Differ 2010; 17:1882–1895.
24. Imai H, Fukutomi J, Kimura A, Fujiwara H. Effect of reduced pressure on the polarization of ^{129}Xe in the production of hyperpolarized ^{129}Xe gas: development of a simple continuous flow mode hyperpolarizing system working at pressures as low as 0.15 atm. Concepts Magn Reson 2008; 33B: 192–200.
25. Imai H, Kimura A, Hori Y, et al. Hyperpolarized ^{129}Xe lung MRI in spontaneously breathing mice with respiratory gated fast imaging and its application to pulmonary functional imaging. NMR Biomed 2011; 24:1343–1352.
26. Ruppert K, Brookeman JR, Hagspiel KD, Mugler JP. Probing lung physiology with xenon polarization transfer contrast (XTC). Magn Reson Med 2000; 44:349–357.
27. Li S, Yang X, Li W, et al. N-acetylcysteine downregulation of lysyl oxidase activity alleviating bleomycin-induced pulmonary fibrosis in rats. Respiration 2012; 84:509–517.
28. Peng R, Sridhar S, Tyagi G, et al. Bleomycin induces molecular changes directly relevant to idiopathic pulmonary fibrosis: a model for "active" disease. PLoS ONE 2013; 8:e59348.
29. Babin AL, Cannet C, Gérard C, Wyss D, Page CP, Beckmann N. Noninvasive assessment of bleomycin-induced lung injury and the effects of short-term glucocorticosteroid treatment in rats using MRI. J Magn Reson Imaging 2011; 33:603–614.
30. Han Y, Englert JA, Yang R, Delude RL, Fink MP. Ethyl pyruvate inhibits nuclear factor-kappaB-dependent signaling by directly targeting p65. J Pharmacol Exp Ther 2005; 312: 1097–1105.
31. Wang CM, Jiang M, Wang HJ. Effect of NF-κB inhibitor on high-mobility group protein B1 expression in a COPD rat model. Mol Med Rep 2013; 7:499–502.
32. Ebina M, Taniguchi H, Miyasho T, et al. Gradual increase of high mobility group protein b1 in the lungs after the onset of acute exacerbation of idiopathic pulmonary fibrosis. Pulm Med 2011; 2011:916486.
33. Li L, Li D, Xu L, et al. Total extract of Yupingfeng attenuates bleomycin-induced pulmonary fibrosis in rats. Phytomedicine 2015; 22:111–119.
34. Yang R, Zhu S, Tonnessen TI. Ethyl pyruvate is a novel anti-inflammatory agent to treat multiple inflammatory organ injuries. J Inflamm (Lond) 2016; 13:37.